14th International Symposium on Turbulence and Shear Flow Phenomena (TSFP14)
Heidelberg, Germany, July 28–31, 2026

NUMERICAL SIMULATION OF SPRAY COMBUSTION USING INTERFACE-RESOLVED COMPRESSIBLE EULERIAN/LAGRANGIAN FRAMEWORK

Kenya Kitada
Dept. of Mechanical Engineering and Science
Kyoto University
Kyoto daigaku-Katsura,Nishikyo-ku,
Kyoto, 615-8540, JAPAN
kitada.kenya.87c@st.kyoto-u.ac.jp

Hikaru Arita
Dept. of Mechanical Engineering and Science
Kyoto University
Kyoto daigaku-Katsura,Nishikyo-ku,
Kyoto, 615-8540, JAPAN
arita.hikaru.48v@st.kyoto-u.ac.jp

Ryoichi Kurose
Dept. of Mechanical Engineering and Science
Kyoto University
Kyoto daigaku-Katsura,Nishikyo-ku, Kyoto, 615-8540, JAPAN
kurose.ryoichi.6x@kyoto-u.ac.jp

ABSTRACT

Spray combustion of *n*-decane jets in crossflow is investigated by three-dimensional (3D) numerical simulations using an Eulerian/Lagrangian framework, where the topological change of the gas-liquid interface is considered within the interface-resolved compressible Eulerian framework, while the dispersed droplets are tracked in a Lagrangian manner. The results show that the present numerical simulation reasonably reproduces the spray combustion. Namely, the liquid column breaks up into small droplets, from which the liquid fuel evaporates and the fuel vapor is transported toward the downstream region. And then, the fuel vapor is mixed with the air and undergoes a chemical reaction. Additionally, the distribution of the reaction rates of the two-step global reactions can be explained by the atomization of the liquid column, evaporation from the interface, and mixing of the fuel vapor with the air. Furthermore, the fuel vapor mass fraction increases in the vicinity of the atomized large droplets and ligaments torn from the liquid column due to the evaporation at their interfaces, which can influence the subsequent ignition.

INTRODUCTION

Spray combustion using liquid fuel has been widely utilized in gas turbine engines of various industrial applications such as aircraft and automobiles. However, it is a highly complex phenomenon where multiple elementary processes such as atomization of liquid fuel, evaporation, mixing with air, and chemical reactions, take place simultaneously and interact with each other. To elucidate its mechanism, numerous experiments (Thomas *et al.* (2019); Lowe *et al.* (2019)) and numerical simulations (Kitano *et al.* (2016); Meng *et al.* (2025)) have been conducted. Although experimental studies can provide insights into what really happens, optical observation inside the combustion chamber tends to be restricted by the harsh operating conditions with high pressure and temperature. Specifically, an optical access to the atomization region near the nozzle is limited, where a dense spray can be formed by breakup of the liquid column into droplets. On the other hand, owing to the rapid development of technologies for high-performance computing, numerical simulations have been paid attention to for clarifying the detailed mechanism.

Typically, the previous numerical studies have used the Eulerian-Lagrangian framework to simulate such a multi-scale phenomenon with affordable computational costs, where the fuel vapor and surrounding gas are treated in an Eulerian manner, while liquid fuel is assumed to be fully atomized and its injection and tracking are conducted in a Lagrangian manner. However, for the fuel injection, the droplet diameter distribution has to be determined in advance by adjusting parameters referring to experimental data or theoretical solutions, which poses questions on their applicability to a wide range of injection conditions. On the other hand, interface-resolved compressible frameworks for multiphase flows (Jemison *et al.* (2014); Fuster & Popinet (2018); Wenzel & Arienti (2023)) have been proposed, where the topological change of the gas-liquid interface of the liquid column and large droplets are directly captured by utilizing the interface-capturing method within the Eulerian manner. However, due to the modeling complexity and prohibitive computational cost, they have not been applied to spray combustion simulations that comprehensively cover all the elementary processes from atomization to chemical reactions, and detailed mechanisms of the interations among the elementary processes have yet to be elucidated.

Therefore, the present study aims to clarify spray combustion of *n*-decane jets in crossflow by three-dimensional numerical simulations in the interface-resolved compressible Eulerian/Lagrangian framework with the two-step global reaction model (Franzelli *et al.* (2010)), where the atomization of the liquid fuel, the evaporation from the interface, and chemical reactions of the fuel vapor are considered in an Eulerian framework, while the evaporation of the dispersed particles that are transformed from the unresolved Eulerian droplets is considered in a Lagrangian framework. Specifically, the effect of

the atomization of the liquid column on the evaporation of the atomized droplets and subsequent chemical reactions are investigated in detail.

NUMERICAL METHODS

An Eulerian/Lagrangian framework is adopted to perform 3D numerical simulations of multi-scale spray combustion with an affordable computational cost, using an in-house thermal flow analysis code based on the finite volume method, developed from FK^3 (Kurose (2026)). The topological change of the gas-liquid interface and the phase change are considered using the volume-of-fluid (VOF) method within the interface-resolved, compressible Eulerian framework (Wenzel & Arienti (2023)), while the dispersed droplets are tracked in the Lagrangian manner. The details of the Eulerian and Lagrangian frameworkds are described in the following sections individually. The other details that are not presented here can be found in our previous works (Kitada & Kurose (2024); Kitada *et al.* (2025)).

Eulerian framework

Governing equations The governing equations are the following conservation equations of the volume fraction, mass, momentum, species mass fraction, and energy.

$$\frac{\partial}{\partial t}\begin{pmatrix}\phi_m\\ \rho_m\phi_m\\ \rho\boldsymbol{u}\\ \rho_g Y_k\phi_g\\ \rho_m E_m\phi_m\end{pmatrix}+\nabla\cdot\begin{pmatrix}\phi_m\boldsymbol{u}_m\\ \rho_m\phi_m\boldsymbol{u}_m\\ \Sigma_m[\boldsymbol{u}_m\otimes\rho_m\phi_m\boldsymbol{u}_m]+p\boldsymbol{I}-\tau\\ \left[\rho_g Y_k\boldsymbol{u}_g+\boldsymbol{q}_{Y,k}\right]\phi_g\\ \left[\rho_m E_m\boldsymbol{u}_m+p\boldsymbol{u}-\boldsymbol{u}\cdot\tau+\boldsymbol{q}_{E,m}\right]\phi_m\end{pmatrix}=\begin{pmatrix}\phi_m\nabla\cdot\boldsymbol{u}_m\\ 0\\ \boldsymbol{F}_{st}\\ \dot{\omega}_k\\ 0\end{pmatrix}+\begin{pmatrix}0\\ S_\rho\\ S_{\rho\boldsymbol{u}}\\ S_{\rho Y_k}\\ S_{\rho E}\end{pmatrix}\delta_{mg}. \tag{1}$$

Here, m is the phase, and $m=l$ and $m=g$ indicates the liquid and gas phases, respectively. ϕ is the volume fraction, $\boldsymbol{u}$ the velocity, ρ the density, p the pressure, $\boldsymbol{I}$ the idenity tensor, τ the viscous stress tensor, Y_k the mass fraction of the kth chemical species, E the total energy comprised of the internal and kinetic energies, σ the surface tension coefficient, and $\boldsymbol{F}_{st}$ the surface tension force. $\dot{\omega}_k$ is the reaction rate of kth chemical species and described later.

$\boldsymbol{q}_{Y,k}$ and $\boldsymbol{q}_{E,m}$ indicates the diffusion of the kth chemical species of the gas phase and thermal diffusion of the phase m, respectively, and are expressed by the following equation.

$$\boldsymbol{q}_{Y,k}=\rho_g Y_k\boldsymbol{V}_k, \tag{2}$$

$$\boldsymbol{q}_{E,m}=-\lambda_m\nabla T_m+\rho_g\Sigma_k h_k Y_k\boldsymbol{V}_k\delta_{mg}. \tag{3}$$

Here, λ is the thermal conductivity, T the temperature, and h the enthalpy. δ_{mg} is the Kronecker delta, implying that the second terms on the right-hand side of Eqs. 1 and 3 are applied only to the gas phase. $\boldsymbol{V}_k$ is the diffusion velocities and replaced by the Hirschfelder-Curtiss approximation as follows.

$$\boldsymbol{V}_k X_k=-D_k\nabla X_k, \tag{4}$$

$$D_k=\frac{1-Y_k}{\Sigma_{j\neq k}X_j/D_{jk}}, \tag{5}$$

where X_k is the mole fraction of species k, and D_{jk} is the binary mass diffusion coefficient of species j into species k.

S_ρ, $S_{\rho\boldsymbol{u}}$, $S_{\rho Y_k}$, and $S_{\rho E}$ represent the interactions between the gas phase and dispersed droplets, and can be computed using the Particle-Source-In-Cell (PSI-Cell) method (Crowe *et al.* (1977); Kitada & Kurose (2024)).

Reaction model For the reaction of n-decane, the two-step global reaction model (Franzelli *et al.* (2010)) for kerosene is used as follows.

$$\mathrm{KERO}+10\mathrm{O_2}\Rightarrow 10\mathrm{CO}+10\mathrm{H_2O}, \tag{6}$$

$$\mathrm{CO}+0.5\mathrm{O_2}\Leftrightarrow\mathrm{CO_2}. \tag{7}$$

Lagrangian framework

Governing equations Atomized Eulerian droplets satisfying conditions of their size and sphericity are transformed into Lagrangian particles. The governing equations for the generated Lagrangian particle's position, velocity, temperature, and mass, are given as follows.

$$\frac{\mathrm{d}\boldsymbol{x}_d}{\mathrm{d}t}=\boldsymbol{u}_d, \tag{8}$$

$$\frac{\mathrm{d}\boldsymbol{u}_d}{\mathrm{d}t}=\frac{f_1}{\tau_d}(\boldsymbol{u}-\boldsymbol{u}_d), \tag{9}$$

$$\frac{\mathrm{d}T_d}{\mathrm{d}t}=\frac{\mathrm{Nu}}{3\mathrm{Pr}}\left(\frac{c_p}{c_{p,d}}\right)\left(\frac{f_2}{\tau_d}\right)(T-T_d)+\frac{\dot{m}_d}{m_d}\frac{L_V}{c_{p,d}}, \tag{10}$$

$$\frac{\mathrm{d}m_d}{\mathrm{d}t}=\dot{m}_d. \tag{11}$$

Here, τ_d is the response time for the droplet, T the ambient temperature, Nu the Nusselt number, Pr the Prandtl number, $c_{p,d}$ the droplet's specific heat capacity at constant pressure, and L_V the latent heat at the droplet temperature T_d. f_1 and f_2 are the correction coefficients for evaporating fuel droplets of Stokes drag force and heat transfer (Kurose *et al.* (2003); Watanabe *et al.* (2007)), respectively. The evaporation rate $\dot{m}_d$ is calculated using a non-equilibrium Langmuir–Knudsen evaporation model (Miller *et al.* (1998); Miller & Bellan (1999); Kitano *et al.* (2014)) as follows.

$$\dot{m}_d=-\frac{m_d}{\tau_d}\left(\frac{\mathrm{Sh}}{3\mathrm{Sc}}\right)\ln(1+\mathrm{B_M}), \tag{12}$$

where Sh is the Sherwood number, Sc the Schmidt number, and $\mathrm{B_M}$ the mass transfer number.

Table 1: Calculation conditions regarding whether the evaporations from the Eulerian gas-liquid interfaces and Lagrangian particles are considered.

	Euler	Lagrange
Case 1	w/	w/
Case 2	w/o	w/

Computational setup

In this study, 3D numerical simulations of spray combustion of liquid fuel jet in crossflow are performed, using the Eulerian/Lagrangian framework. Fig. 1 shows the shematic of the computational domain and conditions. The air crossflow comes into the domain from the y-z plane with the temperature of 760 K and the velocity of 50 m/s. The liquid fuel is assumed to be n-decane ($C_{10}H_{22}$) and injected through the nozzle with a diameter d_{inj} of 0.2 mm from the bottom wall. The dimensions in the x-, y-, and z-directions are 50.0 mm, 5.7 mm, and 5.5 mm, which correspond to $250d_{\mathrm{inj}}$, $28.5d_{\mathrm{inj}}$, and $27.5d_{\mathrm{inj}}$, respectively. The domain consists of 1000, 320, and 360 grid points in the x-, y-, and z-directions, respectively, which corresponds to the total number of the grid points of approximately 0.12 billions. To avoid unphysical reflection from the outflow boundaries, instead of establishing the sponge zone, Navier-Stokes characteristic boundary conditions (NSCBC) (Poinsot & Lele (1992); Lodato *et al.* (2008); Raynaud *et al.* (2015)) are imposed for the outflow boudary, namely, the boundary located in the positive direction of the x-axis. For the spanwise directions, the no-slip condition is imposed on the bottom wall, while the slip condition is imposed except for the bottom wall. The computational domain and conditions have been determined based on the previous numerical study (Kitano *et al.* (2016)). Unlike the previous study where Lagrangian particles are injected into the domain with experiment-based droplet diameter distributions, the liquid n-decane ($C_{10}H_{22}$) is directly injected through the nozzle in the present study. Additionally, the ambient pressure is set to 2 MPa which is larger than the value used in the previous study, which makes the liquid/gas density ratio small enough to keep the simulation stable. Two cases are performed, whose calculation conditions are shown in Table 1. Case 1 considers the evaporations from both the Eulerian gas-liquid interfaces and Lagrangian particles, while Case 2 considers only the evaporation from the Lagrangian particles.

RESULTS AND DISCUSSION

Fig. 2 shows that the instantaneous iso-surfaces of the VOF function $C = 0.5$ and fuel vapor mass fraction $Y_F = 0.001$ in the vicinity of the nozzle in Cases 1 and 2. In both cases, under the influence of the incoming crossflow, the liquid column breaks up into numerous droplets, and some droplets are transformed into Lagrangian particles colored in yellow. Additionally, in Case 1, iso-surfaces of the fuel vapor mass fraction colored in red can be observed around the large droplets and ligaments in the upstream region, which shows that evaporation takes place at the Eulerian gas-liquid interface. On the other hand, in Case 2 where only the evaporation of the Lagrangian particles is considered, the red iso-surfaces can be observed mainly in the downstream region.

To investigate the effect of the evaporation on the subsequent chemical reactions, the instantaneous distributions of the mass fractions of chemical species on the central x-y plane in Cases 1 and 2 are shown in Figs. 3 and 4, respectively. Focusing on the mass fraction of $C_{10}H_{22}$, in Case 1, it tends to be high at the location of the non-dimensionalized x-coordinate x/d_{inj} from 40 to 50 due to the active evaporation from the large droplets and ligaments as shown in Fig. 2(a), while in Case 2, it is lower than that in Case 1. In the further downstream region, it decreases in both cases due to mixing with the incoming crossflow. On the other hand, the mass fractions of the other chemical species gradually increase in the downstream region, although their values are still quite small. The generation of these chemical species is due to the reactions (Eqs. (6) and (7)). Figs. 5 and 6 show the instantaneous distributions of the reaction rates of the two reactions. Q_1 and Q_2 are the reaction rates for reactions (Eqs. (6) and (7)), respectively. Both Q_1 and Q_2 gradually increase in the downstream region in Cases 1 and 2. Additionally, Q_1 in the vicinity of the large droplets and ligaments torn from the liquid column in Case 1 is higher than that in Case 2 due to the evaporation from their interfaces, which can cause the subsequent ignition.

Although the present results are at the very initial stage of the combustion, all the elementary processes of spray combustion such as the atomization of the liquid column, evaporation from the interface, mixing of the fuel vapor with the air, and the chemical reactions are reasonably reproduced with the interface-resolved, compressible Eulerian/Lagrangian framework.

CONCLUSIONS

Spray combustion of n-decane jets in crossflow was investigated by 3D numerical simulations with the Eulerian/Lagrangian framework, using an in-house thermal flow analysis code FK^3. Specifically, the topological change of the gas-liquid interface was considered within the interface-resolved, compressible Eulerian framework, while the dispersed droplets were tracked in a Lagrangian manner. Two cases with or without the evaporation from the Eulerian interface were performed, while both cases considered the evaporation from the Lagrangian particles. The results showed that the present numerical simulation reasonably reproduced the spray combustion. Namely, the liquid column broke up into small droplets and ligaments, from which the liquid fuel evaporated and the fuel vapor was transported toward the downstream region. And then, the fuel vapor was mixed with the air and underwent the chemical reaction. Additionally, it was also found that the distribution of the reaction rates of the two-step global reactions could be explained by the atomization of the liquid column, evaporation from the interface, and mixing of the fuel vapor with the air. Furthermore, the fuel vapor mass fraction increased in the vicinity of the atomized large droplets and ligaments torn from the liquid column due to the evaporation at their interfaces, which could influence the subsequent ignition.

ACKNOWLEDGEMENT

The authors are grateful to Dr. Everett Wenzel of the University of Minnesota for many useful discussions. This work was partially supported by JST SPRING, Grant Number JPMJSP2110 and JSPS KAKENHI, Grant Number 25KJ1589. This work used computational resources of supercomputer Fugaku provided by the RIKEN Center for Computational Science (Project ID:hp240534).

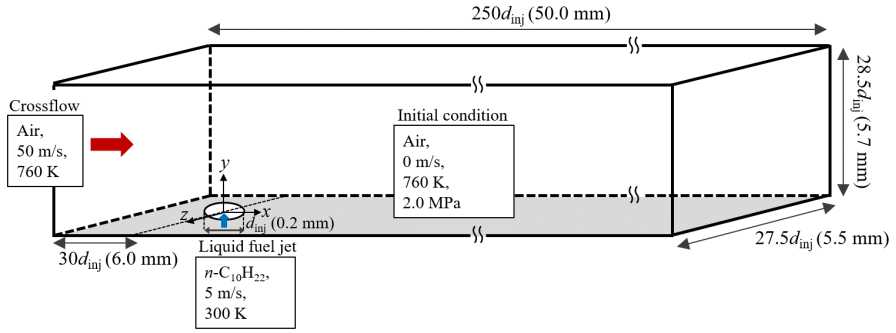

Figure 1: Schematic of the computational domain and conditions.

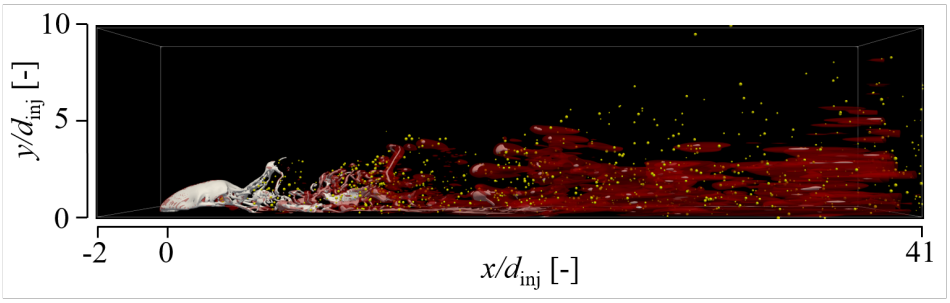

(a) Case1

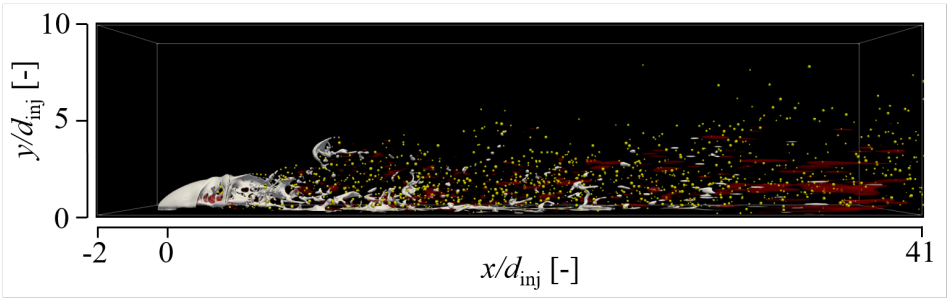

(b) Case2

Figure 2: Snapshots of the instantaneous iso-surfaces of the liquid volume fraction $\phi_l = 0.5$ (gray) and fuel vapor mass fraction $Y_F = 0.005$ (red) in (a) Case 1 and (b) Case 2. The yellow particles represent Lagrangian particles.

REFERENCES

Crowe, Clayton T, Sharma, M Pt & Stock, David E 1977 The particle-source-in cell (psi-cell) model for gas-droplet flows. *Journal of Fluids Engineering* **99**, 325–332.

Franzelli, Benedetta, Riber, E, Sanjosé, M & Poinsot, Thierry 2010 A two-step chemical scheme for kerosene–air premixed flames. *Combustion and Flame* **157** (7), 1364–1373.

Fuster, Daniel & Popinet, Stéphane 2018 An all-mach method for the simulation of bubble dynamics problems in the presence of surface tension. *Journal of Computational Physics* **374**, 752–768.

Jemison, Matthew, Sussman, Mark & Arienti, Marco 2014 Compressible, multiphase semi-implicit method with moment of fluid interface representation. *Journal of Computational Physics* **279**, 182–217.

Kitada, Kenya & Kurose, Ryoichi 2024 High-fidelity numerical simulations in eulerian/lagrangian framework for liquid fuel jets in crossflow with atomization and evaporation: Effect of aerodynamic weber number. *International Journal of Multiphase Flow* **174**, 104762.

Kitada, Kenya, Wei, Tianyi, Iwashita, Takeshi & Kurose, Ryoichi 2025 Surface wettability effect on atomization and evaporation of wall-impinging liquid fuel jets in crossflow. *Physics of Fluids* **37** (3).

Kitano, Tomoaki, Kaneko, Keisuke, Kurose, Ryoichi & Komori, Satoru 2016 Large-eddy simulations of gas-and liquid-fueled combustion instabilities in back-step flows. *Combustion and Flame* **170**, 63–78.

Kitano, Tomoaki, Nishio, Jun, Kurose, Ryoichi & Komori, Satoru 2014 Effects of ambient pressure, gas temperature and combustion reaction on droplet evaporation. *Combustion and Flame* **161** (2), 551–564.

Kurose, Ryoichi 2026 FK^3. http://www.tse.me.kyoto-u.ac.jp/members/kurose/link\LY1\textbackslash_e.php.

Kurose, Ryoichi, Makino, Hisao, Komori, Satoru, Nakamura, Mariko, Akamatsu, Fumiteru & Katsuki, Masashi 2003 Effects of outflow from the surface of a sphere on drag, shear lift, and scalar diffusion. *Physics of fluids* **15** (8), 2338–2351.

Lodato, Guido, Domingo, Pascale & Vervisch, Luc 2008

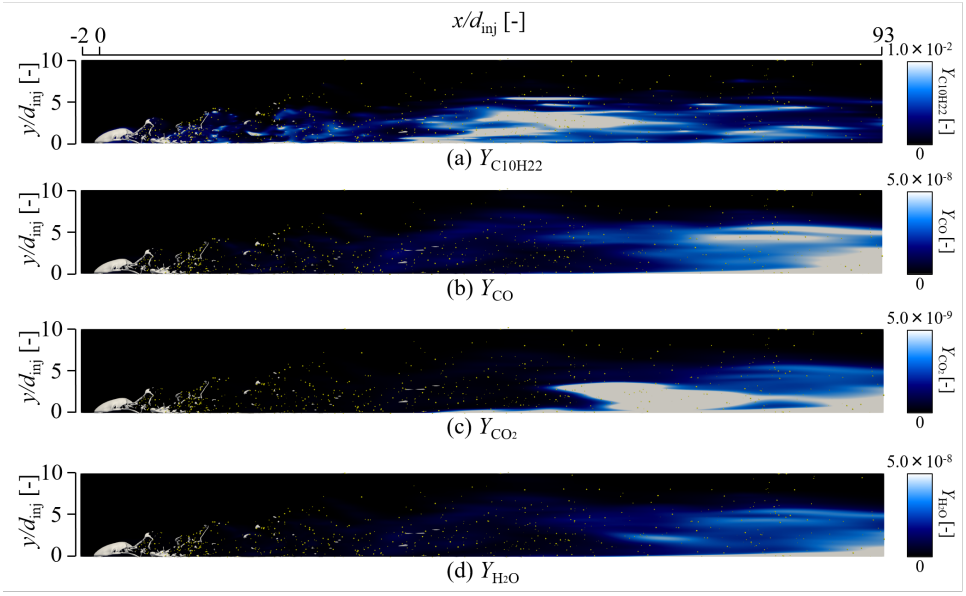

Figure 3: Instantaneous distributions of the mass fractions of (a) $Y_{C_{10}H_{22}}$, (b) Y_{CO}, (c) Y_{CO_2}, and (d) Y_{H_2O}, on the central x-y plane at $t = 0.59$ ms in Case 1. The gray iso-surfaces represent the gas-liquid interfaces captured in the Eulerian framework.

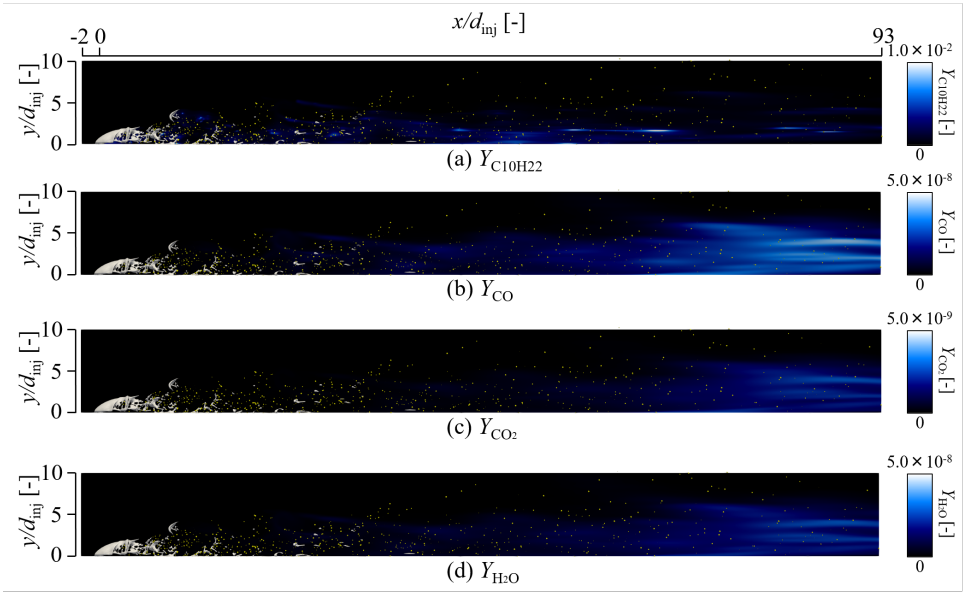

Figure 4: Instantaneous distributions of the mass fractions of (a) $Y_{C_{10}H_{22}}$, (b) Y_{CO}, (c) Y_{CO_2}, and (d) Y_{H_2O}, on the central x-y plane at $t = 0.59$ ms in Case 2. The gray iso-surfaces represent the gas-liquid interfaces captured in the Eulerian framework.

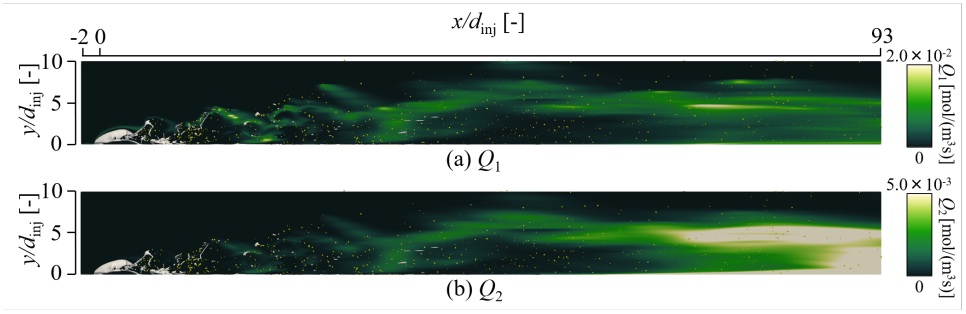

Figure 5: Instantaneous distributions of the reaction rates for (a) the first reaction (Eqs. (6)) Q_1 and (b) second reaction (Eqs. (7)) Q_2 on the central x-y plane at $t = 0.59$ ms in Case 1. The gray iso-surfaces represent the gas-liquid interfaces captured in the Eulerian framework.

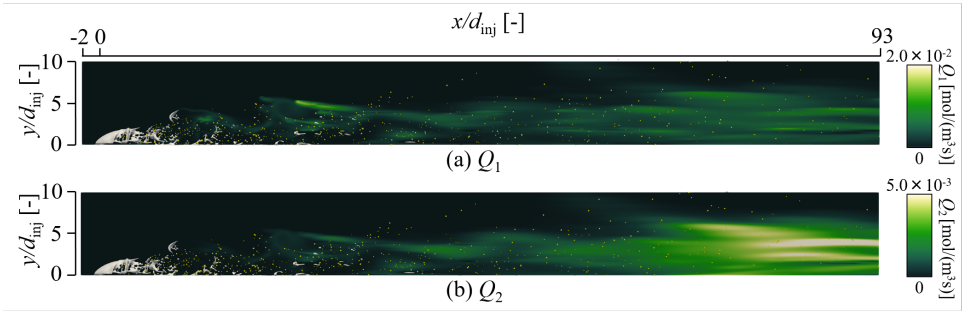

Figure 6: Instantaneous distributions of the reaction rates for (a) the first reaction (Eqs. (6)) Q_1 and (b) second reaction (Eqs. (7)) Q_2 on the central x-y plane at $t = 0.59$ ms in Case 2. The gray iso-surfaces represent the gas-liquid interfaces captured in the Eulerian framework.

Three-dimensional boundary conditions for direct and large-eddy simulation of compressible viscous flows. *Journal of computational physics* **227** (10), 5105–5143.

Lowe, Albyn, Thomas, Levi M, Satija, Aman, Lucht, Robert P & Masri, Assaad R 2019 Five khz thermometry in turbulent spray flames using chirped-probe-pulse femtosecond cars, part ii: Structure of reaction zones. *Combustion and Flame* **200**, 417–432.

Meng, Qian, Wang, Haiou, Chang, Zhuchuan, Cheng, Mengzhen, Huang, Ziwei, Luo, Kun & Fan, Jianren 2025 Direct numerical simulation studies of spray jet flames in hot vitiated crossflow. *Fuel* **389**, 134543.

Miller, RS, Harstad, K & Bellan, J 1998 Evaluation of equilibrium and non-equilibrium evaporation models for many-droplet gas-liquid flow simulations. *International Journal of Multiphase Flow* **24** (6), 1025–1055.

Miller, Richard S & Bellan, J 1999 Direct numerical simulation of a confined three-dimensional gas mixing layer with one evaporating hydrocarbon-droplet-laden stream. *Journal of Fluid Mechanics* **384**, 293–338.

Poinsot, T J & Lele, SK 1992 Boundary conditions for direct simulations of compressible viscous flows. *Journal of computational physics* **101** (1), 104–129.

Raynaud, Félix, Eggels, Ruud LGM, Staufer, Max, Sadiki, Amsini & Janicka, Johannes 2015 Towards unsteady simulation of combustor-turbine interaction using an integrated approach. In *Turbo Expo: Power for Land, Sea, and Air*, , vol. 56642, p. V02BT39A004. American Society of Mechanical Engineers.

Thomas, Levi M, Lowe, Albyn, Satija, Aman, Masri, Assaad R & Lucht, Robert P 2019 Five khz thermometry in turbulent spray flames using chirped-probe pulse femtosecond cars, part i: Processing and interference analysis. *Combustion and Flame* **200**, 405–416.

Watanabe, Hiroaki, Kurose, Ryoichi, Hwang, Seung-Min & Akamatsu, Fumiteru 2007 Characteristics of flamelets in spray flames formed in a laminar counterflow. *Combustion and Flame* **148** (4), 234–248.

Wenzel, Everett A & Arienti, Marco 2023 A conservative, interface-resolved, compressible framework for the modeling and simulation of liquid/gas phase change. *Journal of Computational Physics* **477**, 111957.